PHYSICAL REVIEW D **94,** 113010 (2016)

Suppression of cosmological sterile neutrino production by altered dispersion relations

Elke Aeikens,[1] Heinrich Päs,[2] Sandip Pakvasa,[3] and Thomas J. Weiler[4]

[1]*University of Vienna, Faculty of Physics, Boltzmanngasse 5, A-1090 Vienna, Austria*
[2]*Fakultät für Physik, Technische Universität Dortmund, 44221 Dortmund, Germany*
[3]*Department of Physics & Astronomy, University of Hawaii, Honolulu, Hawaii 96822, USA*
[4]*Department of Physics and Astronomy, Vanderbilt University, Nashville, Tennessee 37235, USA*

(Received 22 June 2016; published 19 December 2016)

Early Universe cosmology imposes stringent bounds on light sterile neutrinos mixing with the active flavors. Here we discuss how altered dispersion relations can weaken such bounds and allow compatibility of new sterile neutrino degrees of freedom with early Universe cosmology and particular a successful generation of the light elements in the early Universe.

DOI: 10.1103/PhysRevD.94.113010

Additional gauge singlet "sterile" neutrinos with masses in the eV range have been discussed as solutions to various neutrino oscillation anomalies, including the appearance of antielectron neutrinos in an antimuon neutrino beam at Liquid Scintillator Neutrino detector [1], the appearance of electron neutrinos in a muon neutrino beam at MiniBooNE [2], the deficit of electron neutrinos in 19 short baseline reactor experiments [3] and the disappearance of electron neutrinos in the GALLEX and SAGE calibration runs with Cr-51 and Ar-37 [4], (for a global analysis see [5]). Moreover, the absence of an upturn in the solar neutrino spectrum at low energies in several solar neutrino experiments has been advocated as evidence for a sterile neutrino with a mass in the milli- to centi-eV range [6]. Such sterile neutrinos are, however, somewhat in conflict with the nonobservation of neutrino disappearance at other reactor or accelerator experiments [7]. Most recently, the IceCube experiment reported a bound on active-sterile neutrino oscillations at energies up to 20 TeV which is in conflict with the parameter space of these hints [8]. At present there are more than 20 experimental neutrino oscillation projects under development or consideration to clarify these puzzling anomalies (see, e.g., [9]).

On the other hand, additional neutrino degrees of freedom contribute to the radiation content in the early Universe and thus lead to a faster expansion and consequently a higher temperature for the weak interaction freeze out. This results in a larger neutron abundance, and consequently a larger Helium abundance. The excellent agreement of the predicted primordial abundances of light elements, in particular of Helium-4, with observations are one of the major successes of big bang cosmology. That this process does not spoil the successful prediction of the observed primordial element abundances poses a stringent bound on the number of neutrino species present in the early Universe (at $T \sim \mathrm{MeV}$) (see, e.g., [10,11]). On the other hand, Ref. [12] has concluded that a fourth thermalized sterile neutrino is favored rather than excluded by big bang nucleosynthesis (BBN) data, while two sterile neutrinos are ruled out at 95% C.L. With the scheme discussed here for the BBN era, any number of sterile neutrinos may be accommodated. Moreover, while the discussion of BBN bounds has gone back and forth, a sterile neutrino population in the early Universe affects other cosmological data as well, in particular the redshift of the radiation-matter equality and its impact on the cosmic microwave background (CMB) [13]. A recent analysis of both BBN and CMB data obtained an upper bound of $\Delta N_{\mathrm{eff}} < 0.2$ at 95% C.L. for the effective number of additional neutrino degrees of freedom in the early Universe [14].

It is thus interesting to explore mechanisms that suppress the sterile neutrino production in the early Universe. One such possibility is provided by matter effects, which can be enhanced, e.g., by a lepton asymmetry reducing the active-sterile neutrino mixing, and consequently also the sterile neutrino production from neutrino oscillations [15]. In a manner similar to the matter effects due to a lepton asymmetry, altered dispersion relations (ADR) can also result in a suppression of sterile-active mixing, and thus to a suppression of the population of sterile neutrinos before the freeze out of weak interactions; thus light sterile neutrinos may become compatible with BBN and other cosmological data. In this paper we analyze quantitatively this effect of ADRs, and find a favorable consequence for sterile neutrino model building. We here concentrate on BBN, but the general mechanism of ADR suppression of early Universe sterile neutrino production is applicable to other processes as well.

A simple but sufficiently accurate estimate of the ^{4}He abundance $Y(^4\mathrm{He})$ in terms of the neutron-to-proton ratio n/p determines the temperature of big-bang nucleosynthesis T_{BBN} [16]:

$$Y(^4\mathrm{He}) = \frac{2n_n/n_p}{1 + n_n/n_p}, \tag{1}$$

where

$$n_n/n_p \simeq \exp\left[-\Delta m_{np}/T_{\rm BBN} + (\mu_e - \mu_{\nu_e})/T_{\rm BBN}\right], \quad (2)$$

with Δm_{np} being the mass difference between n and p, and μ_e, μ_{ν_e} being the chemical potentials of the electron e^- and electron-neutrino ν_e. The reaction rates for the back-and-forth conversion of neutrons and protons are

$$\nu_e + n \leftrightarrow p + e^- \quad \text{and} \quad \overline{\nu}_e + p \leftrightarrow n + e^+. \quad (3)$$

The rates for the two processes in (3) sum up to a rate

$$\Gamma_{\rm BBN} = 2\langle n_e \sigma(E_e, p_e)|v_e|\rangle \quad (4)$$

where n_e is the electron or ν_e particle number density, σ is the reaction cross section for either process in (3), and $|v_e|$ is the relative lepton speed, and fall out of equilibrium for [16,17]:

$$\Gamma_{\rm BBN}(T) \lesssim H(T), \quad (5)$$

with the Hubble parameter given by

$$H(T, g_{\rm eff}^{1/2}) = \left(\frac{8\pi \mathrm{G}}{3}\rho_R\right)^{1/2} = \left(\frac{8\pi^3}{90}\right)^{1/2} g_{\rm eff}^{1/2}\frac{T^2}{m_{\rm Pl}}. \quad (6)$$

Here G denotes Newton's constant, $\mathrm{G} = m_{\rm Pl}^{-2}$ with $m_{\rm Pl}$ being the Planck mass, and $g_{\rm eff}$ is the effective number of degrees of freedom at temperature T. The temperature $T_{\rm BBN}$ is determined when the reaction rate equals the Hubble parameter in Eq. (5).

The introduction of sterile neutrinos affects these processes in two ways. First, the effective number of degrees of freedom $g_{\rm eff}$ will be increased so that the Hubble parameter in Eq. (6) is increased as well. And second, the sterile neutrinos will affect the number density and energy of active neutrinos ν_a ($a = e, \mu, \tau$) and thus also the reaction rate $\Gamma_{\rm BBN}$ in Eq. (4). (As we will assume the sterile neutrino to be decoupled during the process of BBN we will not discuss this possibility further).

A change in the Hubble parameter would in turn alter the temperature $T_{\rm BBN}$, and thus, via the neutron-to-proton ratio, alter the observed light element abundances. This consequence can be avoided if sterile neutrinos ν_s would be kept out of equilibrium before the onset of big bang nucleosynthesis, suppressing their production. This either imposes stringent limits on the $\nu_s - \nu_a$ oscillation parameters $(\theta, \Delta m^2)$ or requires new physics, for example a lepton asymmetry or new neutrino interactions [18] increasing the neutrino matter effect, which suppresses the effective mixing.

In this paper we demonstrate that an analogous suppression can be obtained by considering a third scenario in which the simple, ultrarelativistic dispersion relation

$$E \simeq p + m^2/2p \quad (7)$$

is altered (ADRs) by an additional term $A^{\rm ADR}$ for sterile neutrinos. The most simple realization is to assume different propagation speeds for active and sterile neutrinos, with

$$A^{\rm ADR}(T) = \pm\epsilon E = \pm 3.151\epsilon T \quad (8)$$

added to Eq. (7). The sign of the term indicates Lorentz violating reduction or enhancement, respectively, as it arises in sterile neutrino shortcuts in extra dimensions or refraction, respectively (note the sign difference to [19]). We note that Coleman and Glashow have advocated the equivalence of species-specific limiting-velocities and (species-specific) Lorentz violation. [20].

As a consequence, the effective neutrino masses and mixing are altered in a way similar to what happens when neutrinos propagate inside matter. In fact, the new Lorentz violating ADR term $A^{\rm ADR}$ and the matter potential in the early Universe [21]

$$A^{\rm matter}(T) = \xi_a T^5 = \sqrt{2} G_F n_\gamma (-A_a T^2/M_W^2), \quad (9)$$

add up to the total potential

$$A(T) = A^{\rm matter}(T) + A^{\rm ADR}(T) = \xi_a T^5 \pm 3.151\,\epsilon T, \quad (10)$$

with G_F being the Fermi constant, M_W the mass of the W boson and $n_\gamma = 0.2404 T^3$ the photon density. In contrast to the works [21–23], we assume zero lepton asymmetry or that any lepton asymmetry is negligible and plays no role and set the corresponding term, usually denoted by L_a, to zero. The active-flavor (a) dependent numerical factors A_a are determined by the plasma background at the time of BBN, consisting of neutrons and protons (but negligible antibaryons), equal numbers of electrons and positrons, neutrinos and antineutrinos, and photons which may be neglected as their coupling to neutrinos is so tiny, resulting in $A_e \simeq 55.0$ [21] and $A_{\mu,\tau} \simeq 15.3$ [15,24] (compare also [25]).

As a consequence, the effective two-flavor Hamiltonian in vacuo

$$\mathcal{H} = \frac{\Delta m^2}{4E}\begin{pmatrix} -\cos 2\theta & \sin 2\theta \\ \sin 2\theta & \cos 2\theta \end{pmatrix} \quad (11)$$

describing the active-sterile neutrino oscillations via

$$i\frac{d}{dt}\begin{pmatrix}\nu_a \\ \nu_s\end{pmatrix} = \mathcal{H}\begin{pmatrix}\nu_a \\ \nu_s\end{pmatrix} \quad (12)$$

is altered by an additional term, $\mathcal{H}' = \mathcal{H} + \delta\mathcal{H}$ with

$$\delta\mathcal{H} = \begin{pmatrix} A^{\rm matter} & 0 \\ 0 & -A^{\rm ADR}\end{pmatrix}. \quad (13)$$

The resulting effective two-flavor classical amplitude for oscillation becomes

$$\sin^2 2\tilde{\theta} = \frac{\sin^2(2\theta)}{\sin^2(2\theta) + \cos^2(2\theta)\left(\frac{2E\cdot A(E)}{\Delta m^2 \cos(2\theta)} - 1\right)^2} \tag{14}$$

where the potential energy $A(E)$ now includes both the matter effects of the hot dense early universe as well as an ADR.

The vacuum mixing angle θ by definition occurs at $A(E) = 0$. The resonance condition

$$\left.\frac{2EA(E)}{\Delta m^2 \cos(2\theta)}\right|_{\rm res} = 1 \tag{15}$$

determines the resonance energy. At the resonance energy $E_{\rm Res}$, the additional terms in (13) cancel the difference of the diagonal entries in (11). Note that for energies much smaller than the resonance energy $E_{\rm Res}$, $\mathcal{H}$ dominates $\delta\mathcal{H}$, the change in the dispersion relation decouples, and the scenario discussed resembles the standard vacuum scenario with three active and one sterile neutrino. Note further that for energies much higher than $E_{\rm Res}$, the diagonal term $\delta\mathcal{H}$ dominates $\mathcal{H}$, the ν_s production is highly suppressed, which generates the desired effect in the early Universe, which will be explained in more detail below. Further details of such models have been worked out in [26–30].

The averaged 2-flavor active-sterile oscillation probability is given by

$$\langle P_{\nu_a\to\nu_s}\rangle = \left\langle \sin^2\left(\frac{\Delta\mathcal{H}}{2}t\right)\sin^2(2\tilde{\theta})\right\rangle = \frac{1}{2}\sin^2(2\tilde{\theta}), \tag{16}$$

where $\Delta\mathcal{H}$ is the difference of the $\mathcal{H}$ eigenvalues, equal to $\frac{\Delta\tilde{m}^2}{2E}$.

Following [15], we assume that the initial sterile neutrino density vanishes. The rate of sterile neutrino production is then given by the interaction rate of active neutrinos multiplied with the averaged oscillation probability $\langle P_{\nu_a\to\nu_s}\rangle$, i.e.,

$$\Gamma_{\nu_s} = \langle P_{\nu_a\to\nu_s}\rangle\Gamma_{\nu_a}. \tag{17}$$

The condition that sterile neutrinos do not come into equilibrium then becomes

$$\Gamma_{\nu_s}(T) \lesssim H(T), \tag{18}$$

which has to hold for all temperatures $T > T_{\rm BBN}$. The reaction rates of the active neutrinos are slightly flavor-dependent. The Γ_{ν_a}, with $a = e, \mu, \tau$, are given by [15,31]:

$$\Gamma_{\nu_a} = y_a G_F^2 T^5, \tag{19}$$

where $y_e = 4.0$, $y_{\mu,\tau} = 2.9$.

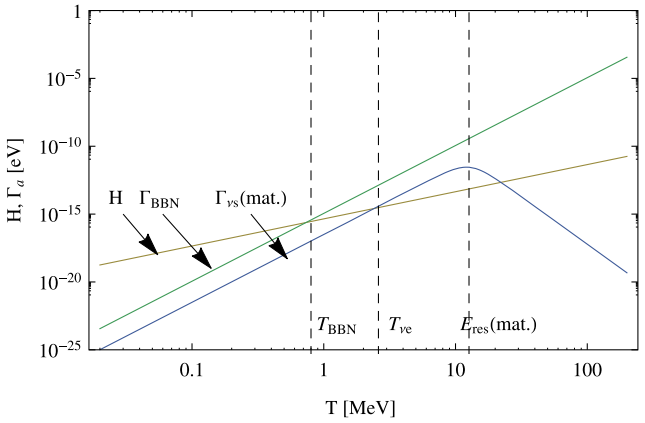

FIG. 1. Reaction rates $\Gamma_{\rm BBN}$, Γ_{ν_s} as a function of temperature in comparison with the Hubble rate H. BBN happens where $\Gamma_{\rm BBN}$ falls below the Hubble rate. Γ_{ν_s} denotes the reaction rate of sterile neutrinos with a matter potential for $\nu_e - \nu_s$ oscillations with $\sin^2\theta = 0.03$, $\Delta m^2 = 0.93$ eV^2.

The reaction rates of active neutrinos freeze out when $\Gamma_{\nu_a} \lesssim H(T)$, i.e., at temperatures $T_e = 2.6$ MeV and $T_{\mu,\tau} = 4.4$ MeV, respectively [15,31].

Figures 1–3 show the resulting sterile neutrino production rate Γ_{ν_s} (blue/dark) for oscillations of electron neutrinos as a function of temperature for an illustrative comparison with the proton-neutron conversion rate $\Gamma_{\rm BBN}$ (green/medium) and the Hubble parameter (yellow/light). (Here, we have set $\sin^2\theta = 0.03$ and $\Delta m^2 = 0.93$ eV^2, corresponding to the best fit data of sterile neutrino oscillations according to [5].)

The crossing point of H with the BBN reaction rate $\Gamma_{\rm BBN}$ defines the temperature $T_{\rm BBN}(\sim 0.8$ MeV) at which BBN ceases to be effective, according to (5). The decoupling temperature of active neutrinos (in these figures the electron neutrinos) lies just above $T_{\rm BBN}$, at $T_{\nu_e} = 2.6$ MeV [15].

Two peaks feature prominently in the sterile neutrino production rates in Fig. 2, where the matter and/or ADR potentials lead to amplified mixing and a change in the functional form which crucially affects the conditions for thermal equilibrium around BBN. While the first (low energy) peak is a real resonance peak, where the effective $\Delta\tilde{m}^2 \equiv 2E\Delta\mathcal{H}$ vanishes, the second (high energy) peak corresponds to the cancellation of matter potential and ADR only. While the resonance condition Eq. (15) is quadratic in energy and thus in principle has two solutions, the number of real positive solutions depends on the sign of Δm^2 and the ADR and matter potentials. We assume the sterile neutrino to be heavier than the active one. Now the matter potential is negative, making active neutrinos effectively even lighter. Thus the only possible resonance arises when a sterile neutrino shortcut cancels the mass difference between active and sterile neutrinos.

Comparing the case for matter effects only (Fig. 1) with the case of matter effects plus an ADR potential (Figs. 2 and 3), one can easily notice the following:

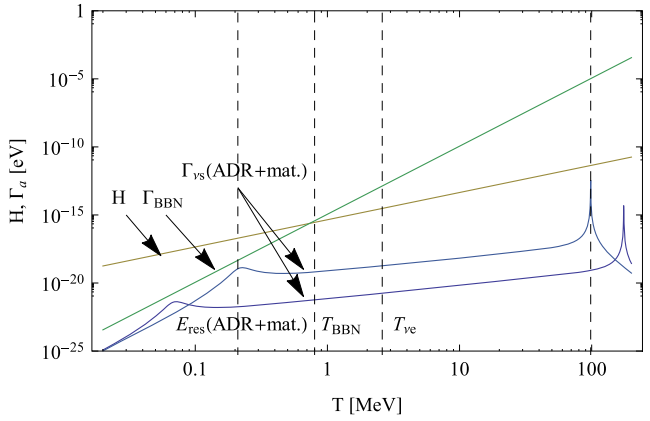

FIG. 2. As above including both a matter potential and an altered dispersion relation due to shortcuts, $A = A^{\mathrm{ADR}} + A^{\mathrm{matter}}$, with $\epsilon = 10^{-12}$ for the upper and $\epsilon = 10^{-11}$ the lower blue (dark) curve, respectively.

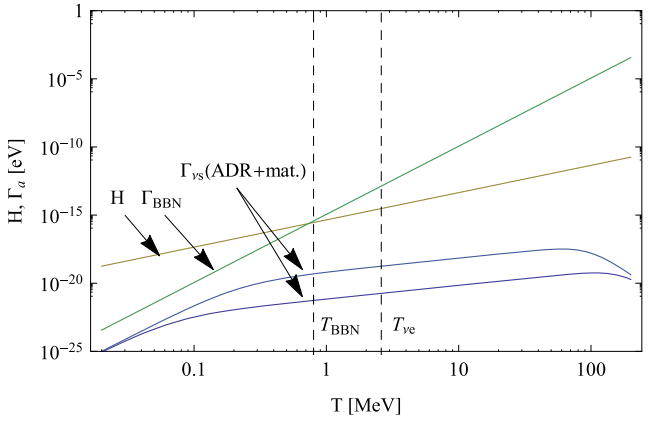

FIG. 3. As above with a negative ADR potential $A = -A^{\mathrm{ADR}} + A^{\mathrm{matter}}$.

(i) In Fig. 1 the resonance of the matter potential lies at $E_{\mathrm{res}}(\mathrm{matter}) = 13$ MeV. Γ_{ν_s} is thus larger than the Hubble rate in the temperature interval $T_{\nu_e} < T < 22$ MeV. In this temperature interval, $\nu_s - \nu_e$ oscillations will populate ν_s. Thus, for this case, condition (18) is violated for $T > T_{\mathrm{BBN}}$.

(ii) In Figs. 2 and 3 the oscillation probability $P_{\nu_e \to \nu_s}$ is shown in the presence of an ADR, with $\epsilon = 10^{-11}, 10^{-12}$, which yields an additional suppression factor of the active-sterile mixing. Note that the ϵ parameters adopted here are several orders of magnitude larger here than the ones discussed in [19,26–30] in the context of short baseline neutrino experiments. This is justified since dramatically different conditions such as larger densities and temperatures prevail in the early Universe which affect the ADRs in the underlying concrete models such as scattering probabilities or spacetime curvature and warp factors. The dependence of ADRs on these conditions is strongly model dependent. The ϵ parameters in the early Universe are thus treated as free with respect to the corresponding low energy bounds.

The cases shown correspond to a suppression (Fig. 2) or an enhancement (Fig. 3) of the sterile neutrino dispersion relation. In Fig. 2, the total potential $A = A^{\mathrm{matter}} + A^{\mathrm{ADR}}$ gives rise to the resonance energies $E_{\mathrm{res}}(\mathrm{matter} + \mathrm{ADR}) \approx 0.2$ MeV and 98.3 MeV ($E_{\mathrm{res}} \approx 0.07$ MeV and 174.8 MeV, respectively). The matter potential is less relevant here since the ADR potential dominates. The maximum of the second resonance peak exceeds the Hubble rate only within the small interval $T = (98.27\text{–}98.33)$ MeV ($T = (174.79\text{–}174.80)$ MeV) which corresponds to a time interval of 2 ns and is less than the oscillation length of about 3 ns (for $\epsilon = 10^{-11}$). Therefore we expect the second resonance peak not to significantly populate sterile number densities. This condition poses another constraint in addition to Eq. (18), i.e., to suppress oscillations in the interval of the resonance peak $T = (T_1 - T_2)$, the oscillation phase $\Phi[T] = \Delta\tilde{m}^2 t/4E$ has to fulfill

$$\Phi[T_2] - \Phi[T_1] < 2\pi. \tag{20}$$

In Fig. 3, $\Gamma_{\nu_s}(T) < H(T)$ is fulfilled everywhere.

To avoid an influence on the expansion rate of the Universe, the production rate of sterile neutrinos and antineutrinos has to be suppressed until the time of BBN T_{BBN}. Thus Eq. (18) in combination with Eqs. (6), (16), (17) and (19), evaluated at T_{BBN} imposes the constraint on the $\nu_s - \nu_a$ oscillation parameters:

$$\sin^2(2\tilde{\theta}) \lesssim \frac{H}{\Gamma_{\nu_a}} = \left(\frac{8\pi^3}{90}\right)^{1/2} \frac{2g_{\mathrm{eff}}^{1/2}}{y_a G_F^2 T^3 m_{\mathrm{Pl}}} \equiv \alpha_a. \tag{21}$$

Here, $g_{\mathrm{eff}} = 10.75$, assuming that the number of degrees of freedom is unaffected by the sterile neutrinos, and we find $\alpha_e \approx 3.20$ and $\alpha_{\mu,\tau} \approx 4.41$. In addition, the condition (20) has to be fulfilled for a positive ADR potential.

Via Eqs. (16) and (21), this implies the following relation between the sterile-active Δm^2 and the vacuum mixing angle $\sin(2\theta)$ (Note that one of the earliest bounds placed on Δm^2 and mixing for a light sterile neutrino from BBN is [32].)

$$\Delta m^2 \leq \frac{2A(T_{\mathrm{BBN}})E(T_{\mathrm{BBN}})}{\cos(2\theta) \pm \sin(2\theta)\sqrt{(1-\alpha_a)/\alpha_a}}. \tag{22}$$

The constraints from (22) and (20) are displayed in Figs. 4 and 5 for $\nu_e - \nu_s$ and $\nu_{\mu,\tau} - \nu_s$ oscillations, respectively, with $\epsilon = 10^{-12}$ and 10^{-11} and in Figs. 6 and 7 for a negative ADR potential. The shaded areas depict the parameter

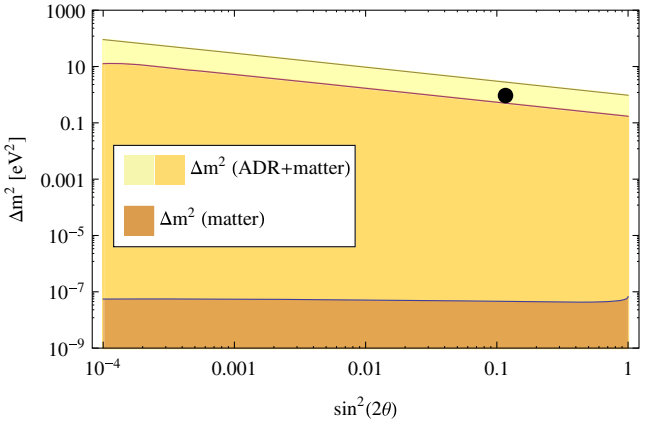

FIG. 4. Comparison of allowed regions (shaded areas) for successful BBN, in the two cases $\nu_s - \nu_e$ neutrino oscillations in matter, and oscillations in the presence of both matter and an ADR potential $A = A^{\rm matter} + \epsilon E$, for a shortcut parameter of $\epsilon = 10^{-12}$ (darker shaded) and $\epsilon = 10^{-11}$ (lighter shaded).

space where sterile neutrinos are not populated and BBN can proceed successfully. The parameter regions above the shaded areas are excluded. In each figure, cases for matter effects only (dark shaded areas), and for a combination of matter effects and an ADR potential (light shaded areas) are shown. In the latter case the allowed region is larger, [$\Delta m^2 \sin^2(2\theta) \lesssim 0.71(0.28)\,\mathrm{eV}^2$ for $\nu_e(\nu_{\mu/\tau})$ with $\epsilon = 10^{-12}$, and $\Delta m^2 \sin^2(2\theta) \lesssim 0.95(1.58)\ \mathrm{eV}^2$ for $\nu_e(\nu_{\mu/\tau})$ with $\epsilon = 10^{-11}$, respectively], since the ADR potential $A^{\rm ADR} = 3.151 \epsilon T_{\rm BBN} \sim 10^{-6}$ eV alone is sufficient to suppress the oscillation amplitude $\sin^2(2\tilde{\theta})$. In the case of pure matter effects ($A^{\rm matter}[T_{\rm BBN}] \sim 10^{-14}$ eV) the allowed region is constrained to $\Delta m^2 \sin^2(2\theta) \lesssim 6.5(1.7) \times 10^{-8}\ \mathrm{eV}^2$ for $\nu_e(\nu_{\mu/\tau})$.

In comparison to the case for $\nu_e - \nu_s$ oscillations shown in Fig. 4, the bounds on $\nu_{\mu,\tau} - \nu_s$ oscillations in Fig. 5 are slightly less stringent due to a larger interaction rate ($\Gamma_{\mu,\tau}/\Gamma_e = 1.38$). Finally the allowed parameter regions

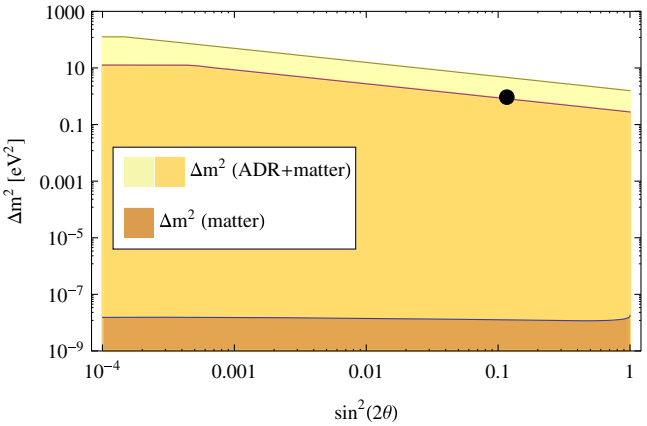

FIG. 5. As above, but for $\nu_s - \nu_{\mu/\tau}$ neutrino oscillations.

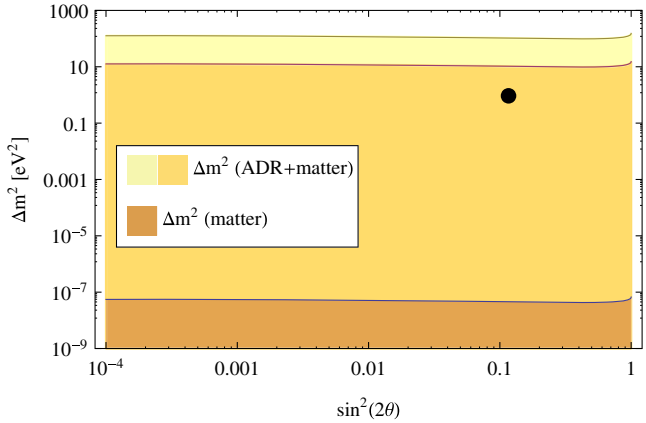

FIG. 6. As above but for $\nu_s - \nu_e$ neutrino oscillations with negative ADR potential, $A = A^{\rm matter} - \epsilon E$.

become even larger when a negative ADR potential (postive refraction of sterile neutrinos) is assumed, as can be seen in Figs. 6, 7.

The black dots correspond to the best fit data of the global neutrino oscillation data analysis including short and long-baseline accelerator, reactor, and radioactive source experiments, as well as atmospheric and solar neutrinos in a $3+1$ scenario [5], with $\sin^2\theta = 0.03$ and $\Delta m^2 = 0.93\ \mathrm{eV}^2$. As can be seen, the global best fit value can be made compatible with successful BBN in the early Universe in all cases by assuming a large enough shortcut parameter ϵ.

Finally, one has to discuss the relevance of the first (low energy) resonance peak in Fig. 2 for the relic neutrino background. In contrast to the high energy peak this peak is a real resonance that can lead to Mikheyev-Smirnov-Wolfenstein (MSW) transitions once the adiabaticity condition

$$\gamma[T_{\rm peak}] = \frac{\tau_{\rm sys}}{\tau_{\rm int}} = \frac{1}{\omega_{\rm eff}} \frac{d\tilde{\theta}}{dt} \ll 1 \qquad (23)$$

is fulfilled. The expression for the adiabaticity parameter [compare [33] with (14)]

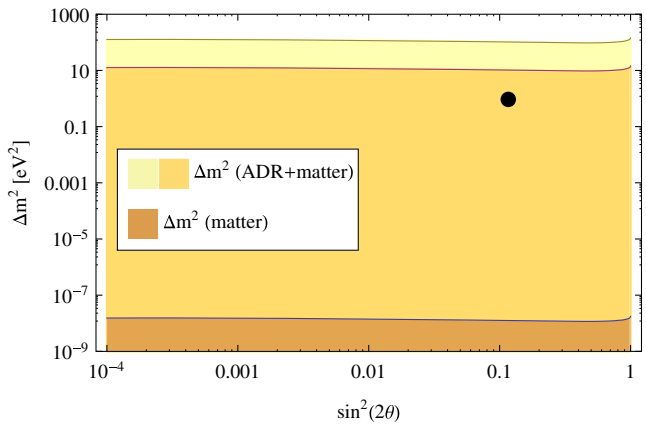

FIG. 7. As above, but for $\nu_s - \nu_{\mu/\tau}$ neutrino oscillations.

$$\gamma = \frac{8(3.151T)^2 \cdot H[T]}{(\Delta m^2)^2} \frac{\sin(2\theta)(A^{\mathrm{ADR}}[T] + 3A^{\mathrm{matter}}[T])}{[\sin^2(2\theta) + (\cos(2\theta) - \frac{A2(3.151T)}{\Delta m^2})^2]^{3/2}} \tag{24}$$

results in $\gamma(\nu_e - \nu_s) \approx 10^{-10}$, $\gamma(\nu_{\mu/\tau} - \nu_s) \approx 10^{-11}$, thus leading to virtually complete MSW conversion with an MSW probability $P_{\nu_a \to \nu_s} \approx 0.97$ which does not significantly depend on $\sin\theta$ and Δm^2. Thus, while this transition is at temperatures low enough not to affect BBN or the total amount of neutrinos in the Universe N_ν anymore, depending on which and how many flavors mix with the sterile neutrino, the scenario predicts a partly or virtually completely sterile relic neutrino background, making the difficult endeavor to detect the neutrino background [34] even more challenging.

In summary, we have demonstrated that ADR potentials yield a suppression of active-sterile neutrino mixing at high energies that has the potential to significantly enhance the parameter space allowed for sterile neutrinos. Thus ADR scenarios such as shortcuts in extra dimensions [19] with an ADR parameter $\epsilon = 10^{-12}, 10^{-11}$ allow an alternative to the case of large lepton asymmetries in order to make sterile neutrinos compatible with early Universe cosmology. We have concentrated here on the case of BBN which can be generalized to other cosmological processes in the early Universe being sensitive on the number of thermalized neutrino species.

ACKNOWLEDGMENTS

A. E. is supported by the Fonds zur Förderung der wissenschaftlichen Forschung Austrian Science Fund under the Doctoral Program No. W1252-N27 Particles and Interactions. The research of T. J. W. is supported in part by Department of Energy Grant No. DE-SC0011981. H. P. is supported by Deutsche Forschungsgemeinschaft Grant No. PA 803/10-1 and thanks the Alexander von Humboldt Foundation, Vanderbilt University and the University of Hawai'i at Manoa for additional financial support.

[1] A. Aguilar-Arevalo *et al.* (LSND Collaboration), Evidence for neutrino oscillations from the observation of $\bar{\nu}_e$ appearance in a $\bar{\nu}_\mu$ beam, Phys. Rev. D **64**, 112007 (2001).
[2] A. A. Aguilar-Arevalo *et al.* (MiniBooNE Collaboration), Improved Search for $\bar{\nu}_\mu \to \bar{\nu}_e$ Oscillations in the MiniBooNE Experiment, Phys. Rev. Lett. **110**, 161801 (2013).
[3] G. Mention, M. Fechner, T. Lasserre, T. A. Mueller, D. Lhuillier, M. Cribier, and A. Letourneau, The reactor antineutrino anomaly, Phys. Rev. D **83**, 073006 (2011).
[4] C. Giunti and M. Laveder, Statistical significance of the Gallium anomaly, Phys. Rev. C **83**, 065504 (2011).
[5] J. Kopp, P. A. N. Machado, M. Maltoni, and T. Schwetz, Sterile neutrino oscillations: The global picture, J. High Energy Phys. 05 (2013) 050.
[6] P. C. de Holanda and A. Y. Smirnov, Solar neutrino spectrum, sterile neutrinos and additional radiation in the Universe, Phys. Rev. D **83**, 113011 (2011).
[7] See, e. g., K. N. Abazajian *et al.*, Light sterile neutrinos: A white paper, arXiv:1204.5379, and references therein. We note Bill Louis's warning, that comparing different experiments, necessarily having different systematics, can be misleading.
[8] (The IceCube Collaboration), Searches for Sterile Neutrinos with the IceCube Detector, Phys. Rev. Lett. **117**, 071801 (2016).
[9] T. Lassere, in BLV 2013, MPI für Kernphysik, Heidelberg (to be published).
[10] M. Pospelov and J. Pradler, Big bang nucleosynthesis as a probe of new physics, Annu. Rev. Nucl. Part. Sci. **60**, 539 (2010).
[11] J. Beringer *et al.* (Particle Data Group Collaboration), Review of particle physics (RPP), Phys. Rev. D **86**, 010001 (2012). See also the partial updates for the 2014 edition on the hompage http://pdg.lbl.gov/.
[12] G. Steigman, Neutrinos and big bang nucleosynthesis, Adv. High Energy Phys. **2012**, 268321 (2012).
[13] S. Gariazzo, C. Giunti, M. Laveder, Y. F. Li, and E. M. Zavanin, Light sterile neutrinos, J. Phys. G **43**, 033001 (2016).
[14] R. H. Cyburt, B. D. Fields, K. A. Olive, and T. H. Yeh, Big bang nucleosynthesis: 2015, Rev. Mod. Phys. **88**, 015004 (2016).
[15] R. Foot and R. R. Volkas, Reconciling Sterile Neutrinos with Big Bang Nucleosynthesis, Phys. Rev. Lett. **75**, 4350 (1995).
[16] E. W. Kolb and M. S. Turner, *The Early Universe* (Westview Press, Boulder, CO, 1994).
[17] M. Trodden and S. M. Carroll, TASI lectures: Introduction to cosmology, arXiv:astro-ph/0401547.
[18] M. Archidiacono, S. Gariazzo, C. Giunti, S. Hannestad, R. Hansen, M. Laveder, and T. Tram, Pseudoscalar—sterile neutrino interactions: reconciling the cosmos with neutrino oscillations, J. Cosmol. Astropart. Phys. 08 (2016) 067.
[19] H. Päs, S. Pakvasa, and T. J. Weiler, Sterile-active neutrino oscillations and shortcuts in the extra dimension, Phys. Rev. D **72**, 095017 (2005).
[20] S. R. Coleman and S. L. Glashow, High-energy tests of Lorentz invariance, Phys. Rev. D **59**, 116008 (1999).
[21] K. Enqvist, K. Kainulainen, and J. Maalampi, Resonant neutrino transitions and nucleosynthesis, Phys. Lett. B **249**, 531 (1990).

[22] A. D. Dolgov, Neutrinos in cosmology, Phys. Rep. **370**, 333 (2002).
[23] D. P. Kirilova and M. V. Chizhov, Cosmological nucleosynthesis and active sterile neutrino oscillations with small mass differences: The resonant case, Nucl. Phys. **B591**, 457 (2000).
[24] D. Notzold and G. Raffelt, Neutrino dispersion at finite temperature and density, Nucl. Phys. **B307**, 924 (1988).
[25] S. Hannestad, I. Tamborra, and T. Tram, Thermalisation of light sterile neutrinos in the early universe, J. Cosmol. Astropart. Phys. 07 (2012) 025.
[26] S. Hollenberg, O. Micu, H. Päs, and T. J. Weiler, Baseline-dependent neutrino oscillations with extra-dimensional shortcuts, Phys. Rev. D **80**, 093005 (2009).
[27] H. Päs, S. Pakvasa, J. Dent, and T. J. Weiler, Closed timelike curves in asymmetrically warped brane universes, Phys. Rev. D **80**, 044008 (2009).
[28] J. Dent, H. Päs, S. Pakvasa, and T. J. Weiler, Neutrino time travel, arXiv:0710.2524.
[29] S. Hollenberg and H. Päs, Resonant active-sterile neutrino mixing in the presence of matter potentials and altered dispersion relations, arXiv:0904.2167.
[30] D. Marfatia, H. Päs, S. Pakvasa, and T. J. Weiler, A model of superluminal neutrinos, Phys. Lett. B **707**, 553 (2012).
[31] K. Enqvist, K. Kainulainen, and M. J. Thomson, Stringent cosmological bounds on inert neutrino mixing, Nucl. Phys. **B373**, 498 (1992).
[32] P. Langacker, Report No. UPR-0401T, 1989.
[33] T. K. Kuo and J. T. Pantaleone, Neutrino oscillations in matter, Rev. Mod. Phys. **61**, 937 (1989).
[34] P. Vogel, How difficult it would be to detect cosmic neutrino background?, AIP Conf. Proc. **1666**, 140003 (2015); G. Drexlin, V. Hannen, S. Mertens, and C. Weinheimer, Current direct neutrino mass experiments, Adv. High Energy Phys. **2013**, 293986 (2013); S. Betts *et al.*, Development of a relic neutrino detection experiment at PTOLEMY: Princeton tritium observatory for light, early-Universe, massive-neutrino yield, arXiv:1307.4738; J. Lesgourgues and S. Pastor, Neutrino cosmology and Planck, New J. Phys. **16**, 065002 (2014).